Supporting Information

Shape-Controlled Synthesis and *In Situ* Characterisation of Anisotropic Au Nanomaterials using Liquid Cell Transmission Electron Microscopy

Shih-Ting Wang[†‡‖], Yiyang Lin[†‡§], Michael H. Nielsen[⊥], Cheng Yu Song[‖], Michael R. Thomas[†‡§], Christopher D. Spicer[†‡§], Roland Kröger[▽], Peter Ercius[‖], Shaul Aloni[‖], and Molly M. Stevens[*†‡§]

[†]Department of Materials, Imperial College London, Exhibition Road, London, SW7 2AZ, United Kingdom

[‡]Department of Bioengineering, Imperial College London, London, SW7 2AZ, United Kingdom

[§]Institute of Biomedical Engineering, Imperial College London, London, SW7 2AZ, United Kingdom

[⊥]Physical & Life Sciences Directorate, Lawrence Livermore National Laboratory, 7000 East Avenue, Livermore, California, 94550, United States

[‖]Molecular Foundry, Lawrence Berkeley National Laboratory, 1 Cyclotron Road, Berkeley, California, 94720, United States

[▽]Department of Physics, University of York, Heslington, YO5 10DD, United Kingdom

Materials. Full-length islet amyloid polypeptide (IAPP-amide, 95 %) was purchased from Cambridge Bioscience. Gold nanoparticles (Au NPs) were purchased from BBI Solutions. Gold chloride ($HAuCl_4$), 4-(2-hydroxyethyl)-1-piperazineethanesulfonic acid (HEPES), sodium phosphate monobasic (NaH_2PO_4), sodium phosphate dibasic (Na_2HPO_4) and Thioflavin T (ThT) were purchased from Sigma-Aldrich (UK). Carbon grid (200 mesh copper) and uranyl acetate solution were purchased from Electron Microscopy Sciences. Silicon nitride (Si_xN_y) TEM grids (15 nm with 9 each 0.1x0.1 mm windows) were purchased from Ted Pella Inc. The Si_xN_y windows for liquid cell transmission electron microscopy (LCTEM) experiments were purchased from Hummingbird Scientific Inc. Milli-Q (18 MΩ · cm) was used for all the experiments.

Preparation of IAPP fibrils. IAPP solution (25 μM) was prepared by dissolving the peptide powder in sodium phosphate buffer (20 mM, pH 7.5). To form mature fibrils,

the solution was aged at room temperature for at least 48 h before follow-up experiments.

TEM imaging of IAPP fibrils. (1) For conventional TEM sample preparation, 10 μL of IAPP fibril solution (25 μM) was dropped on a carbon film for 5 min and the residual liquid was removed with a piece of filter paper. After that, the fibrils were stained with 5 μL of 1 wt % uranyl acetate for 5 min. The excess staining agent was removed with filter papers. (2) For LCTEM, the Si_xN_y grid was prepared by plasma treatment (350−450 mtorr atmosphere for 30 sec) using a plasma sterilizer (Harrick, PDC-32G). Afterward, 5 μL of the fibril solution was dropped on the Si_xN_y grid for 2 min and the residual liquid was removed with a piece of filter paper. TEM imaging was performed on a JEOL 2100F TEM with an acceleration voltage of 200 kV, and the images were recorded by Orius camera.

Liquid cell assembly for LCTEM imaging. Si_xN_y windows with spacer sizes of 100 nm, 250 nm and 1 μm were used for the LCTEM experiments. The window thickness was 30 nm and the lateral dimensions was 30 μm x 200 μm. Prior to cell assembly, the Si_xN_y windows were plasma treated (400-600 mtorr atmosphere for 90 sec) using a plasma sterilizer (Harrick, PDC-32G) to obtain a hydrophilic surface. The cell was assembled with 0.6 μL of deionised water. The sealing quality of the assembled liquid cell was checked in the vacuum station (Hummingbird Scientific Inc.) to ensure no liquid leakage from the cell (*i.e.,* the vacuum state was in the range of 10^{-5}−10^{-6} mbar at a pump speed of 1500 Hz). The holder remained in the station for ~15 min while flowing deionised water at 5 μL/min to ensure the sealing quality and a liquid flow through the channel. To study Au particle growth in the presence of IAPP fibrils, the cell was assembled with 0.6 μL of IAPP fibril solution (50 μM). Here, we used a 250 nm liquid cell to investigate the effect of Au-binding peptide on regulating the anisotropic growth of Au particles. To label the IAPP fibrils, 10 nm Au NP solution (BBI) was diluted to a concentration of ~$2.8x10^{11}$ particles/mL (5% v/v) in deionised water and injected at 1 or 2 μL/min for ~45 min before flowing water.

LCTEM imaging. After the holder (Hummingbird Scientific Inc.) was transferred to the TEM (JEOL 2100F, 200 kV), imaging was first performed to ensure the presence of liquid and absence of contamination in the cell by injecting deionised water at 5 μL/min. Prior to Au reduction, $HAuCl_4$ (1 mM) was injected at 5 μL/min for ~15 min without electron beam radiation for the Au ions (Au^{3+}) to fill the vicinity of the cell and reach equilibrium. Typical Au reduction experiments were performed at selected area

with a condenser aperture of 50 μm (exposure area of 20 μm^2), magnification of 5 kx and current density (J_c) of ~55 pA/cm^2. The electron dose rate was calculated as ~1.78 $e^-/Å^2 \cdot s^{-1}$. The dynamic growth process was recorded with an Orius camera set to an exposure time of 0.2 sec, and using the VirtualDub software to acquire video with a frame rate of 1 frame/sec. All the supplementary movies were accelerated 10.05 times using AVS Video Editor.

TEM imaging of Au particles after *in situ* experiments. TEM, STEM, HRTEM images and SAED patterns (*i.e.,* **Figures 1c−e, 2b−g, S4, S5, S9 and S10**) of the various Au structures were obtained after the *in situ* experiments and performed on a Philips CM300 TEM at 300 kV. Image processing including calculation of Au particle sizes and FFT of the HRTEM images were performed using ImageJ. To index the facets, the *d*-spacing and angles were first measured from the fast Fourier transformed (FFT) images created from selected areas. The parameters were compared with a standard diffraction pattern of fcc structure to index each set of planes.

STEM imaging of branched Au particles. STEM imaging of a branched Au particle from the *in situ* experiments was performed on a Philips CM200 TEM at 200 kV. Images were taken at a step of 1° from -40° to -20°, and 2° from -20 to +36°. The images were stacked and saved in an animated gif format using ImageJ.

Circular dichroism (CD) analyses. IAPP monomer solution was prepared by dissolving the peptide powder in phosphate buffer (20 mM, pH 7.5) just before CD measurement, and the fibrils were obtained by aging the IAPP solution for 48 h prior to the measurement. The samples were loaded in a 0.1 cm quartz cell, and CD spectra were acquired using a Jasco-715 spectrometer, with the scanning speed of 50 nm/min, resolution of 2 nm, data pitch of 0.1 nm, 2 accumulation times, and a response time of 4 sec. The data unit was converted from machine units (milli-degree, θ) into molar ellipticity $[\theta]$ using the equation:

$$[\theta] = \theta / (10 * P * conc.)$$

Where P is the path length in cm and *conc.* is the molar concentration of the peptide samples.

Thioflavin T (ThT) fluorescence assay. IAPP solution (25 μM) was prepared in phosphate buffer (20 mM, pH 7.5) containing 10 μM of ThT in a 384 well-plate. Fluorescence kinetics was measured with Perkin Elmer EnSpire plate reader, with a time interval of 2 min (λ_{ex} = 440 nm and λ_{em} = 485 nm).

Chemical reduction of Au^{3+} in the presence of IAPP fibrils. IAPP fibril solution (100 μM) was obtained by incubating the peptide powder in phosphate buffer (20 mM, pH 7.5) for at least 48 h. To the IAPP solution, $HAuCl_4$ solution and HEPES buffer were added and the final concentrations of $HAuCl_4$, IAPP and HEPES were 200 μM, 10 μM, and 25 mM, respectively. The mixture was left for 2 h at room temperature before TEM sample preparation, and TEM imaging on a JEOL 2100F TEM at an accelerating voltage of 200 kV.

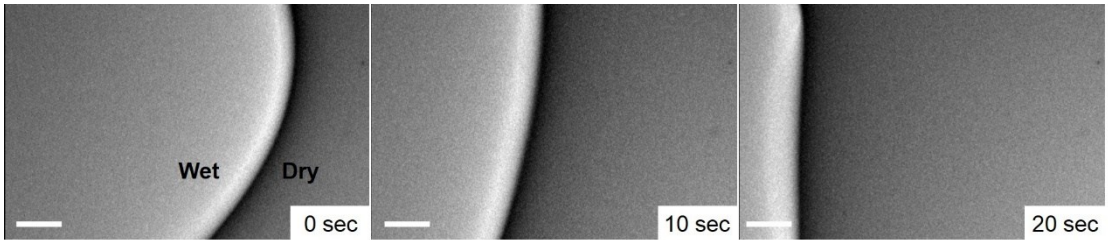

Figure S1 Snapshots show liquid depletion in the LCTEM (100 nm liquid cell) during electron beam exposure (Mag. 3 kx, $J_c \sim 270$ pA/cm^2, dose rate of ~8.74 $e^-/Å^2 \cdot s^{-1}$). Scale bars: 1 μm.

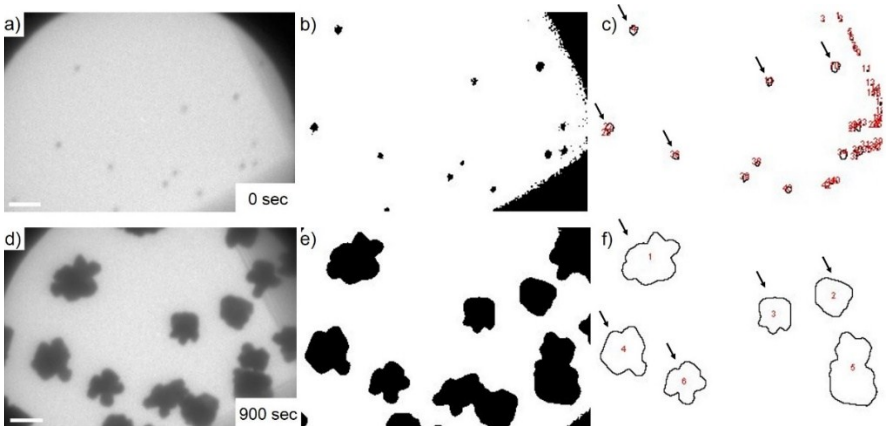

Figure S2 Size analyses of the branched Au particles for plotting the growth trajectory in **Figure 1b** (250 nm liquid cell) were performed using the built-in particle analysis tool in ImageJ. Briefly, the colour threshold of LCTEM images (**Figure S2a, S2d**) was first adjusted to give images **S2b, S2e**; the particle outlines were generated (images **S2c, S2f**) and the surface area of individual particles was analysed. Five Au particles were selected of which no coalescence was observed during the growth processes: (a−c) 0 sec and (d−f) 900 sec. Scale bars: 0.5 μm

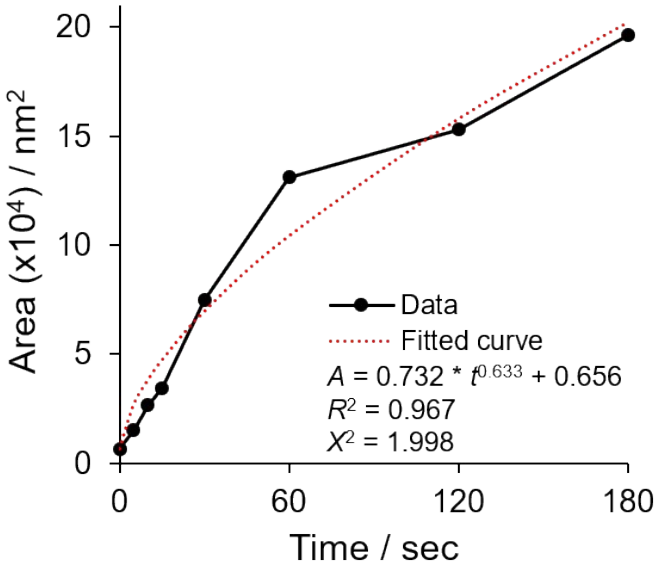

Figure S3 Surface areas of the 2D-projected Au particles plotted against time showing the growth kinetics of the branched structures in **Figure 1a, b**. The growth trajectory was fitted with the power model with pre-set boundaries of a ≥ 0 and 1 ≥ b ≥ 0. Deviation of the fitted curve from the growth trajectory was observed particularly after 180 sec, likely due to confined growth in the *z*-direction and continuous Au^{3+} supply in the open flow system.

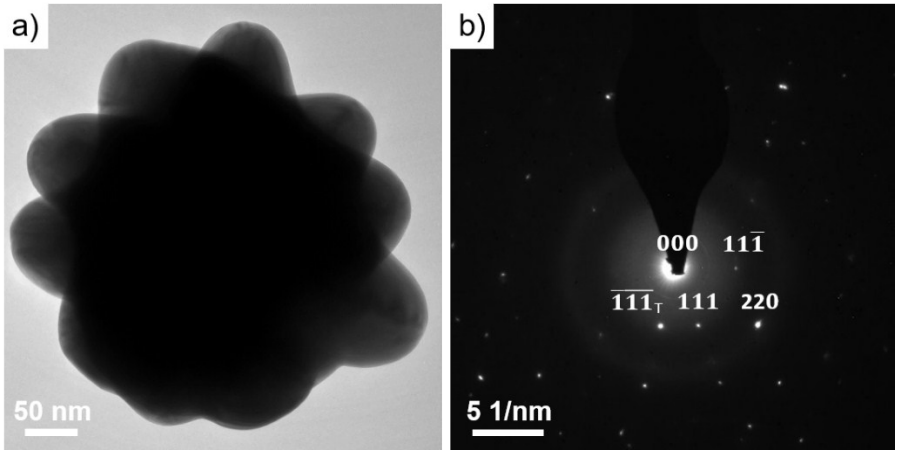

Figure S4 (a) Post-mortem TEM image of the branched Au particle (**Figure 1e**) in TEM mode obtained from an *in situ* experiment in a 250 nm liquid cell. (b) The corresponding SAED pattern shows the presence of twinned facets. However, the diffraction details could not be identified due to the thickness of the particle.

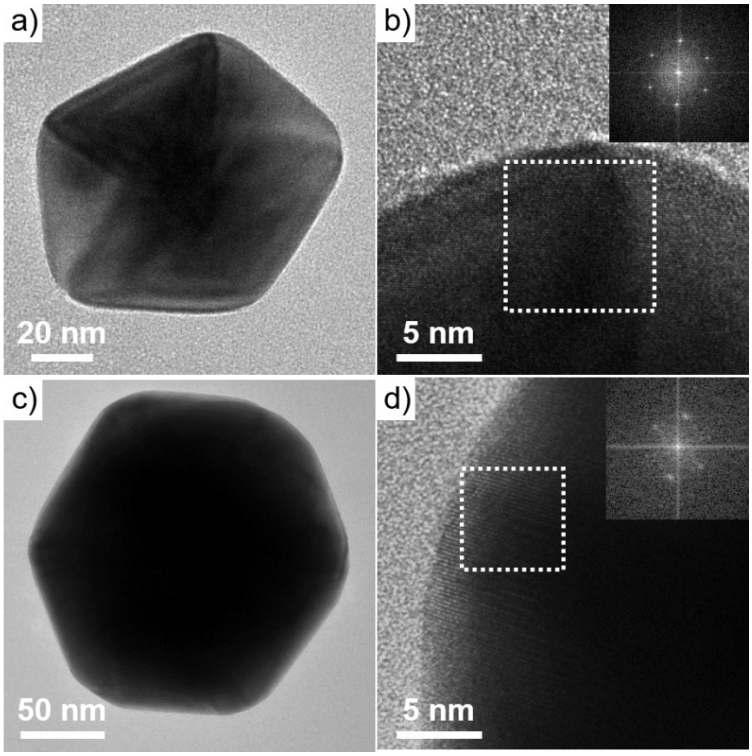

Figure S5 Post-mortem (a, c) TEM, (b, d) HRTEM images and fast Fourier transformation (FFT) of the selected regions of the images (insets of b and d) of the electron beam induced Au seeds formed by *in situ* experiments in a 250 nm liquid cell. The images are supportive of our hypothesis that formation of twinned structures is likely to trigger branched Au particle growth from the twin boundaries.

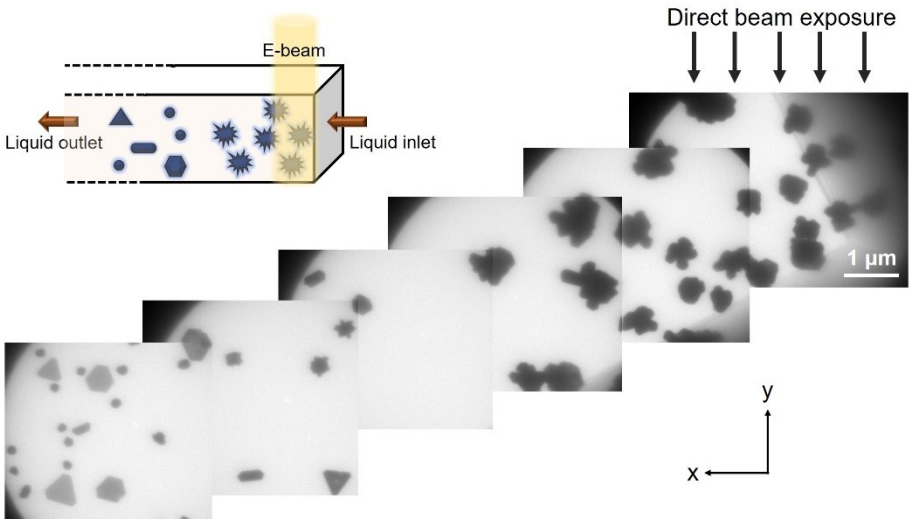

Figure S6 LCTEM images showing different Au morphologies along the liquid flow direction in a 250 nm liquid cell (scale bar: 1 µm). The TEM images were taken at regions perpendicular to the beam path and along the direction of the liquid flow after 15 min of electron beam irradiation at the window corner (image to the right). The

formation of Au particles outside the irradiation area is proposed to be due to the liquid flow that transports e^-_h and radiation-induced Au(0) to these regions. Note that the as-grown Au particles remained adsorbed on the Si_xN_y window during the continuous liquid flow.

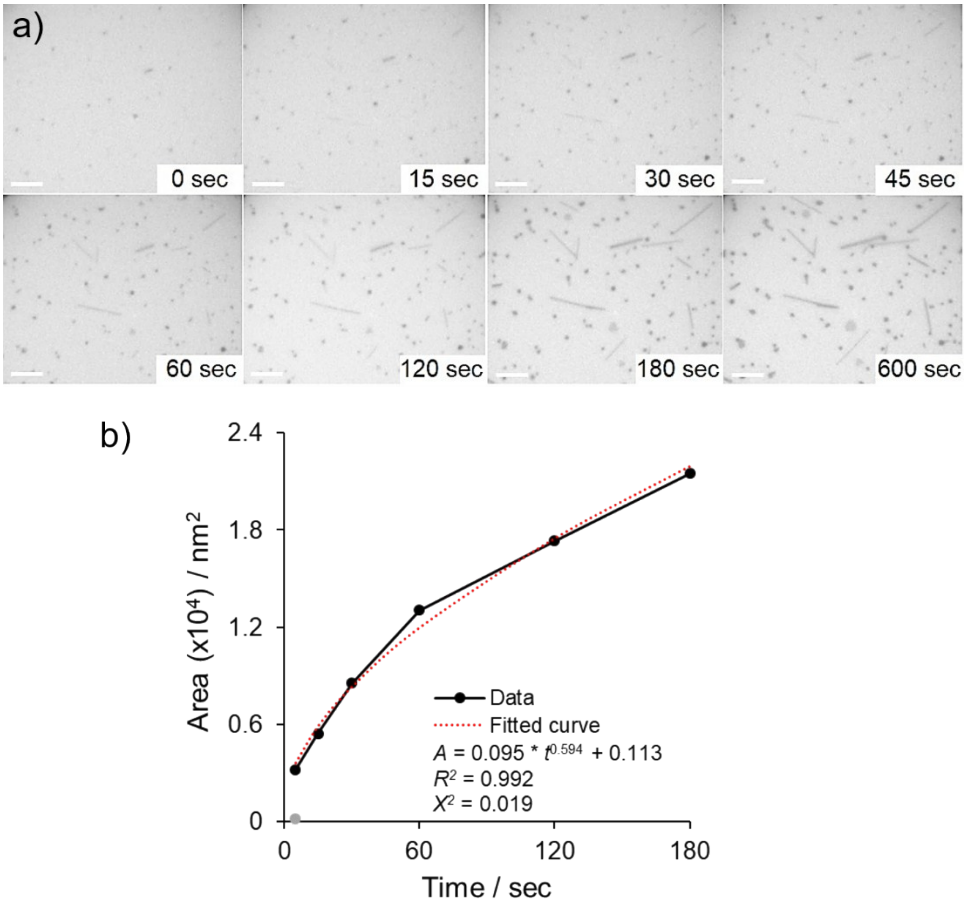

Figure S7 (a) Snapshots of the *in situ* LCTEM experiment show the formation and elongation of Au rods in a 1 μm liquid cell (scale bars: 500 nm). (b) Surface areas of the 2D-projected Au rods plotted against time showed the trend of Au growth in (a). The growth trajectory was fitted with the power model within 180 sec. The fitting was performed with pre-set boundaries of $a \geq 0$ and $1 \geq b \geq 0$.

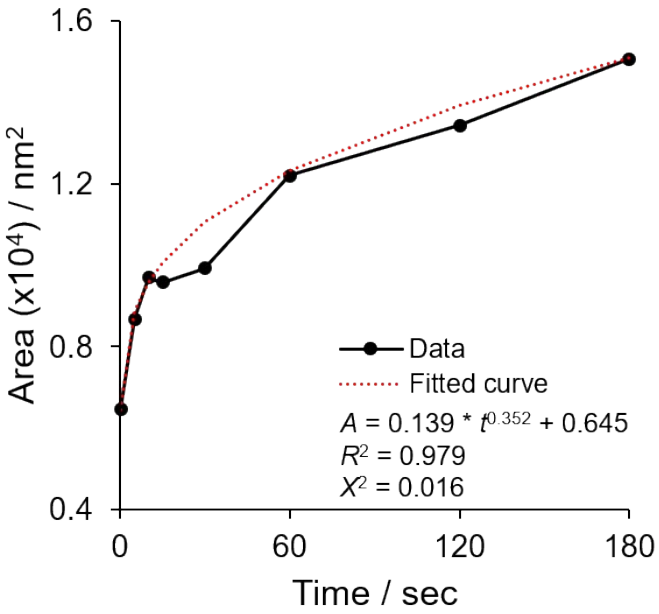

Figure S8 Surface areas of the 2D-projected Au triangles plotted against time showing the trend of Au growth in **Figure 3a and 3c**. The growth trajectory was fitted with the power model within 180 sec. The fitting was performed with pre-set boundaries of $a \geq 0$ and $1 \geq b \geq 0$.

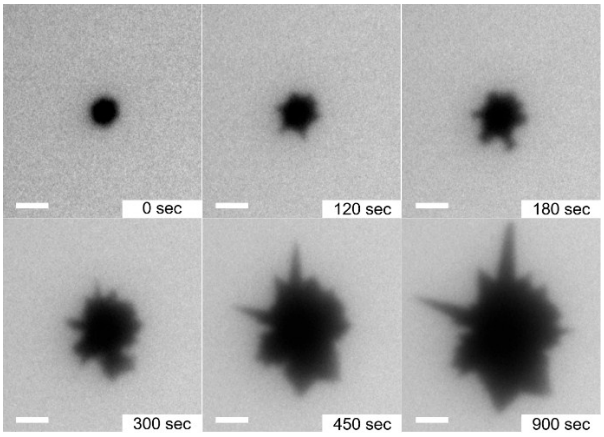

Figure S9 Snapshots of *in situ* LCTEM show the formation of branched Au particles in the 100 nm liquid cell, where growth and splitting of the Au branches were observed. Note that the Au seed particle at 0 sec was pre-formed on the liquid cell window (scale bars: 500 nm).

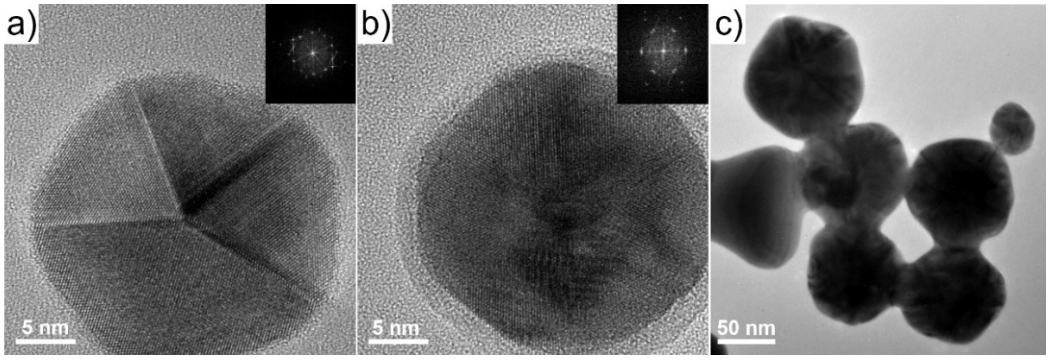

Figure S10 Post-mortem (a, b) HRTEM images, fast Fourier transformation (FFT) of the images (inset of a and b), and (c) TEM images of the electron beam induced Au seeds formed by *in situ* experiments in a 100 nm liquid cell, show the multi-twinned structures that are proposed to trigger branched Au particle growth from the twin boundaries.

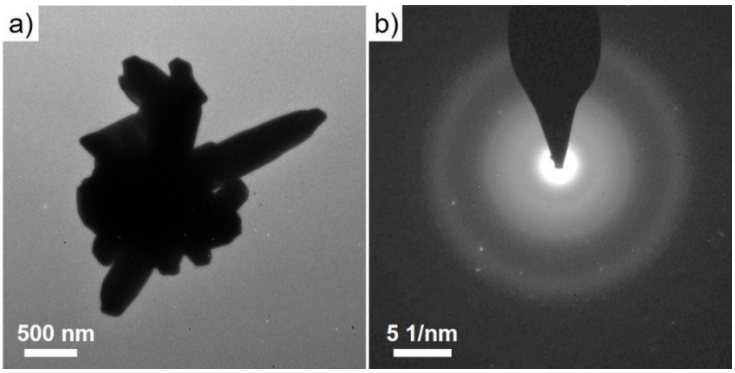

Figure S11 (a) Post-mortem TEM image and (b) the corresponding SAED pattern show the polycrystalline structure of the branched Au particle with sharp tips, formed during an *in situ* LCTEM experiment in a 100 nm liquid cell. However, it was difficult to define the ring diffraction pattern due to the thick Au particle.

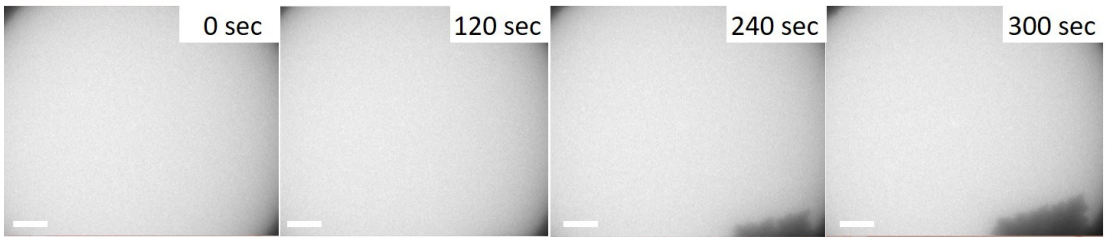

Figure S12 Snapshots of *in situ* LCTEM experiment in a 100 nm liquid cell show no formation of Au seed particles under direct electron beam irradiation. Instead, Au growth was observed to initiate around irradiated area (scale bars: 0.5 μm).

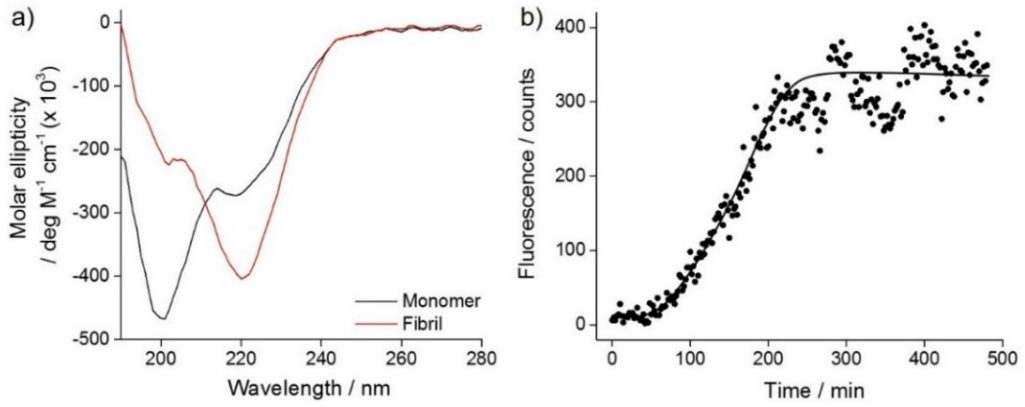

Figure S13 Characterisation of IAPP fibrillation by (a) CD spectroscopy and (b) Thioflavin T assay. (a) IAPP monomer (black spectrum, 25 μM) was measured upon dissolving in sodium phosphate buffer (20 mM, pH 7.5). The solution was left ageing at room temperature for 47 h to obtain mature IAPP fibrils (red spectrum). (b) IAPP (15 μM) fibrillation kinetics were measured at a time interval of 2 min (λ_{ex} = 440 nm and λ_{em} = 485 nm).

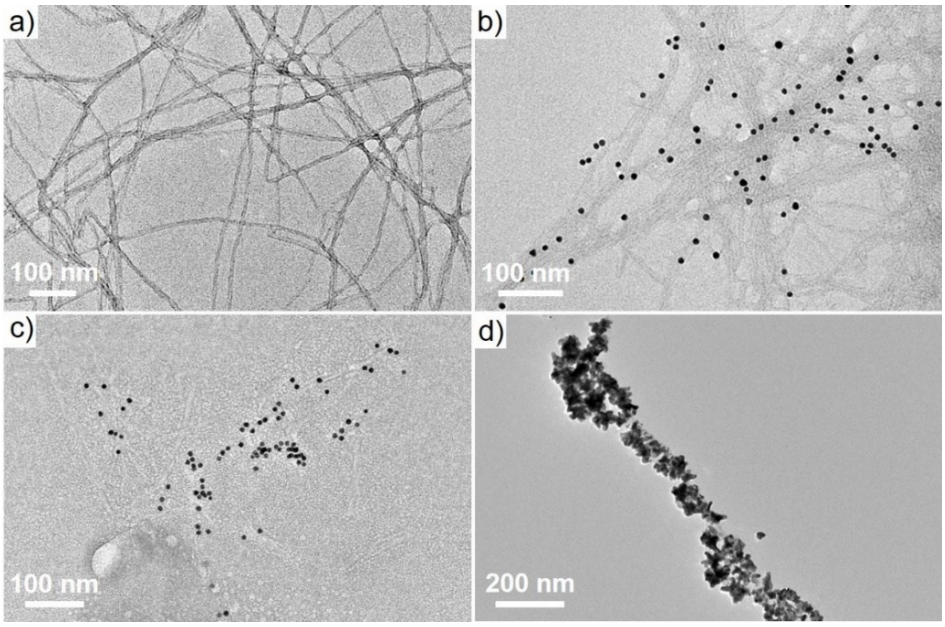

Figure S14 TEM images of IAPP fibrils and the interaction with Au NPs. (a) Mature fibrils, (b, c) alignment of pre-formed Au NPs on fibrils on (b) carbon grid and (c) Si_xN_y grid. (d) Au growth on the fibrils by chemical reduction using HEPES buffer (25 mM, pH 7.5), showing the preferential binding of Au nanoparticles on the fibrillar surface. (a, b, d) Fibrils were negatively stained with uranyl acetate (1 wt%) prior to TEM imaging.

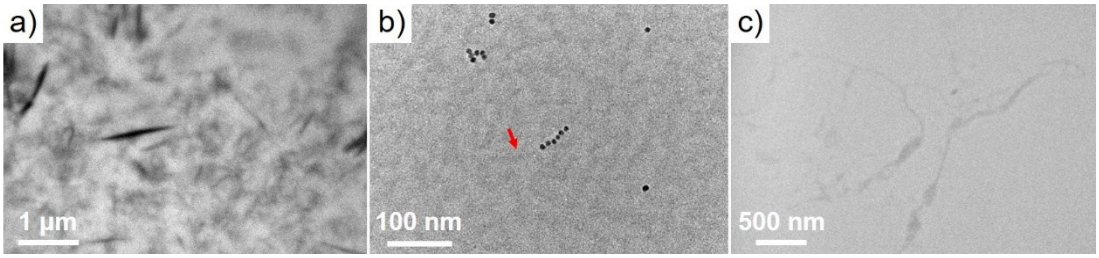

Figure S15 LCTEM images of IAPP fibrils stained with (a) uranyl acetate (1 wt%) and (b) 5 nm Au NPs. The red arrow points at the IAPP fibril underneath the particles. (c) LCTEM image of unstained IAPP fibrils.

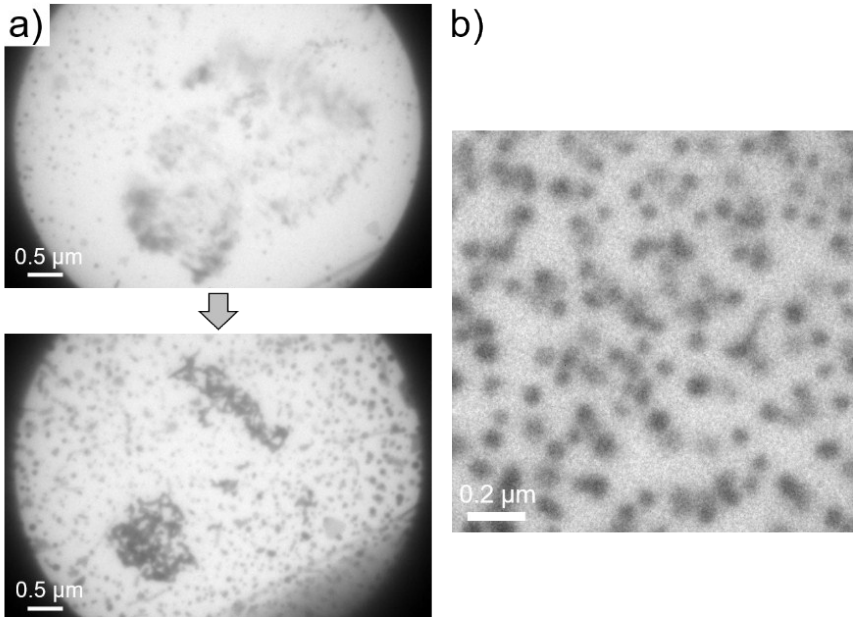

Figure S16 (a) LCTEM images show Au staining of the IAPP fibrils and the denaturing effect of the electron beam in a 250 nm liquid cell. After taking the initial TEM image (top image), Au particle growth and fibril aggregation were observed under the electron beam irradiation (bottom image). (b) LCTEM image of the Au particles formed near the irradiation area after the growth process.

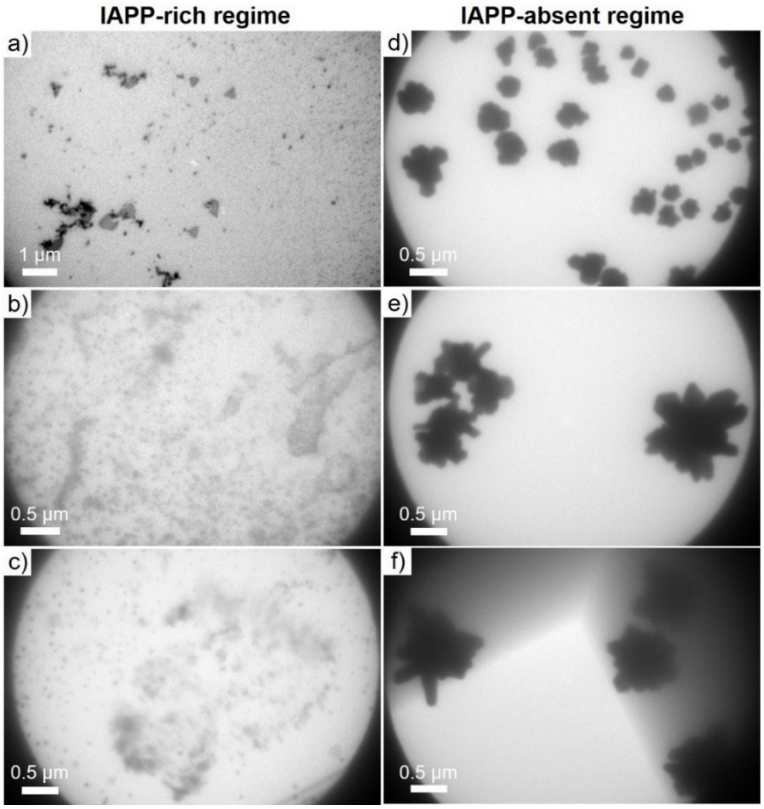

Figure S17 LCTEM images at different locations in the same cell: (a−c) small spherical particles were observed when IAPP fibrils were present, (d−f) branched particles were formed when IAPP fibrils were absent. The thickness of liquid cell is 250 nm.

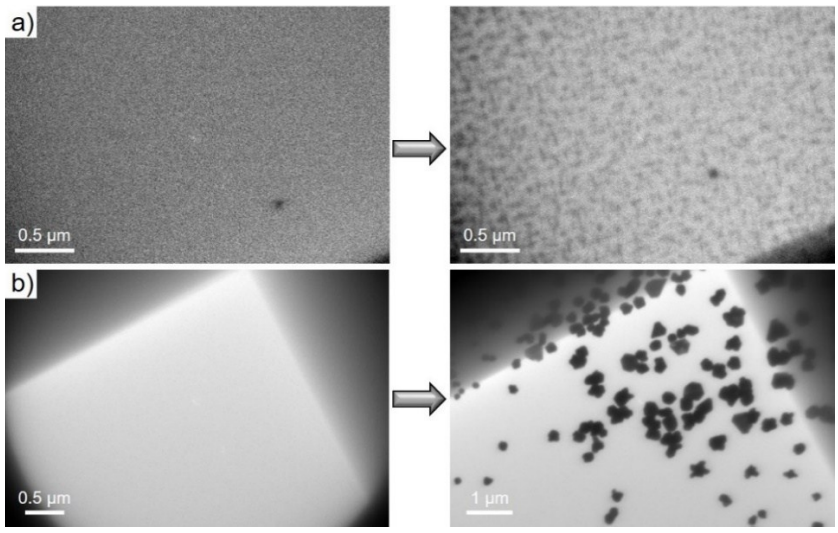

Figure S18 Comparison of the Au growth in LCTEM with (a) and without (b) IAPP fibrils in a 250 nm liquid cell. The left images were taken prior to $HAuCl_4$ injection and Au growth (right images), which confirmed that the cell was filled with liquid and that the window surface was clean.